Experimental Results of Polarimetric Detection Schemes for DVB-T Based Passive Radar

Francesca Filippini [1*], Fabiola Colone [1], Diego Cristallini [2], Georgia Bournaka [2]

[1] Dept. of Information Engineering, Electronics and Telecommunications (DIET), Sapienza University of Rome, Via Eudossiana, 18 - 00184 Rome, Italy
[2] Fraunhofer-Institute for High Frequency Physics and Radar Techniques (FHR), Fraunhoferstr. 20 - 53343 Wachtberg, Germany
[*] francesca.filippini@uniroma1.it

Abstract: This paper investigates the potential advantages conveyed by the exploitation of polarimetric diversity in Passive Coherent Location (PCL) system exploiting Digital Video Broadcasting - Terrestrial (DVB-T) signals. To this purpose, different polarimetric detection schemes are considered that jointly exploit the signals collected at different receiving channels characterized by differently polarized antennas. A performance analysis has been carried using experimental data collected by a passive radar system developed by Fraunhofer, namely PARASOL. This PCL system employs two orthogonal linearly polarized receiving channels (horizontal and vertical). The results obtained against cooperative targets demonstrate that a Polarimetric Generalized Likelihood Ratio Test (P-GLRT) detection scheme provides a remarkable improvement in terms of target detection capability as compared to the single-polarization operation and the non-coherent integration of the results obtained at the available polarimetric channels.

1. Introduction

Thanks to the renewed interest that Passive Coherent Location (PCL) technology has recently received [1]-[3], many signal processing techniques and operative strategies have been developed to make these systems effective in different scenarios. Among the most recently proposed solutions, the exploitation of information diversity conveyed by multiple receiving channels is often considered as a way to increase the system reliability against the many effects that are not under the control of the PCL radar designer. The sought diversity can be gained, for example, from the signals collected by displaced antennas [4]-[6] or at different carrier frequencies [7]-[10] .

Another interesting approach is based on the simultaneous exploitation of the signals collected by differently polarized antennas. Basically, following the consideration that target echoes typically show a random polarization, we observe that the use of a fixed polarization on receive might result in a significant Signal to Noise Ratio (SNR) degradation. It can therefore be expected that a proper combination of the signals received at differently polarized antennas might yield a detection performance improvement for the resulting system. Possible solutions along this line have been investigated in [11]-[15].

In particular, with reference to the target detection stage, a very preliminary polarimetric processing scheme has been firstly investigated in [12] where a simple Non-Coherent Integration (NCI) of the results obtained at cross-polarized surveillance antennas has been proposed for Frequency Modulation (FM) radio based PCL. In [13] it has been shown that, besides the expected improvement due to NCI of target echoes received on multiple channels, polarization diversity might be fruitfully exploited to reject the disturbance contributions that still limit the achievable performance (e.g. cancellation residuals or interfering signals). To this purpose, a Polarimetric-Generalized Likelihood Ratio Test (P-GLRT) detection scheme has been derived to adaptively exploit the polarimetric differences between the target and the competing disturbance. As a consequence, the target discrimination capability can be improved. The proposed approach has been further extended in [14] where the joint exploitation of both frequency and polarimetric diversity has been considered.

The effectiveness of the polarimetric approaches proposed in [12]-[14] has been extensively demonstrated for an FM radio based PCL system. Specifically, the conceived schemes have been shown to be able to mitigate also the effect of co-channel and adjacent-channel interferences arising from the typical spectrum management for FM radio broadcast transmissions (i.e. frequency reuse, broad spectrum roll-off of FM radio signals, etc.).

As is well known, with the advent of digital broadcast services, the interest in studying passive radar applications based on such illuminators has been growing. Digital waveforms present a stationary ambiguity function with a thumb-tack shape and constant bandwidth. Among them, DVB-T represents a very attractive opportunity for PCL applications since it presents good waveform properties for passive radar purposes in terms of both range and Doppler achievable resolution. The successful application of polarization diversity in FM radar based PCL systems, has motivated us to investigate the potential benefits of such polarization diversity in DVB-T based PCL systems.

First experimental results along this line have been reported in [15] for a maritime scenario. The results obtained have shown that, using different polarizations on receive, the target echo was observed with different Signal to Interference plus Noise Ratio (SINR) values. Therefore, the application of a suitable method of combining the signals received at differently polarized channels has been shown to provide the potential for a target detection improvement. However, to this purpose, a simple polarimetric NCI was solely exploited.

In this paper, we extend the work in [15] by comparing different polarimetric detection schemes in DVB-T based PCL systems.

Specifically, also the P-GLRT proposed in [13] is considered in order to successfully exploit the polarization diversity between the target echoes and the competing background. The experimental analysis is performed using data collected by the experimental passive radar system PARASOL developed at Fraunhofer FHR [16]. Particularly, two parallel receiving channels have been employed, connected to two cross-polarized antennas that collect the vertical and horizontal polarized versions of the surveillance signal. The experimental tests included aerial and maritime cooperative targets that enable an effective comparison of the detection performance provided by different polarimetric approaches.

The paper is organized as follows. In Section 2 a basic signal processing scheme of a DVB-T based passive radar is briefly summarized. In Section 3, the polarimetric detection schemes considered in this paper to jointly exploit the signal collected at different polarimetric channels are described. Section 4 illustrates the experimental tests and the data set that has been used to assess the achievable performance. The results obtained are reported in Section 5 together with our detailed comments. Some conclusions are drawn in Section 6.

2. DVB-T based passive radar signal processing scheme

Fig. 1 sketches a basic processing scheme for a DVB-T based PCL system equipped with multiple surveillance channels. Firstly the signals collected by different channels undergo three main processing stages separately as briefly described in sub-sections 2.1, 2.2 and 2.3. Then target detection is performed by exploiting the output of a single channel or by jointly processing the outputs of multiple channels, as described in Section 3.

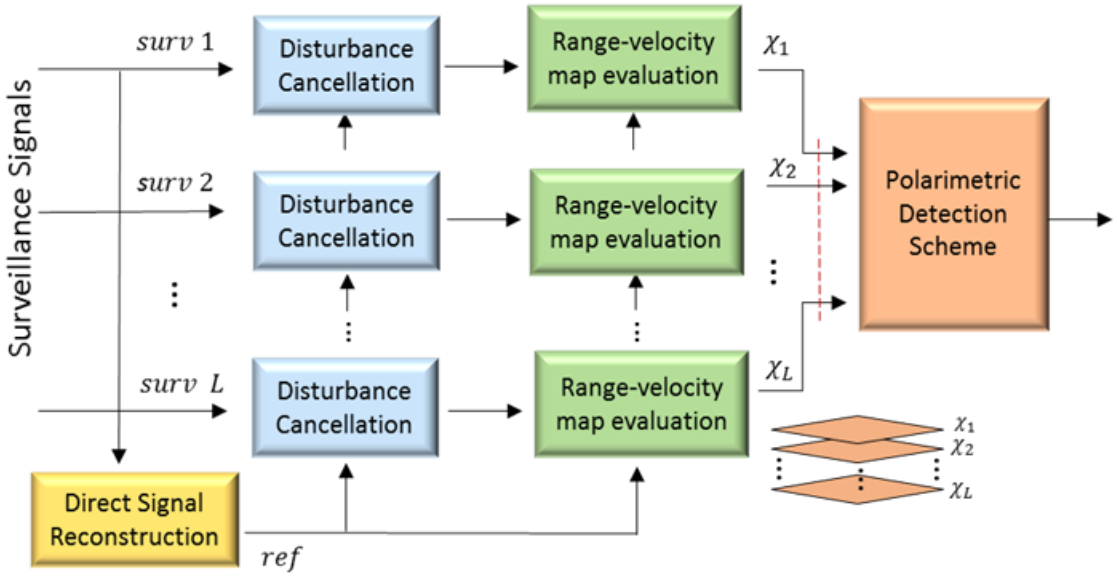

Fig. 1 *Basic processing scheme of a multi-channel DVB-T based PCL system*

2.1. Direct signal reconstruction

In the case of DVB-T signal as Illuminator of Opportunity (IO), due to the digital coding of Orthogonal Frequency Division Multiplexing (OFDM), it is possible to decode the transmitted reference signal. Hence there is no need for a dedicated reference channel. In fact, digitally coded illuminators allow the receiver to reconstruct the transmitted signal by demodulating and remodulating the received signal, according to the DVB-T standard. This operation consists of three main steps: (i) synchronization to the transmitter, (ii) demodulation and decoding of the synchronized signal, (iii) remodulation of the decoded signal. The output of such processing would be a cleaned replica of the direct signal, free of multipath echoes [17], which may be used as reference signal for the following stages. The direct signal reconstruction approach is a valuable solution for reducing the number of receiving channels in a PCL, but it requires a small bit error rate in the decoding of the bit stream, which indirectly calls for a sufficient SNR for the direct signal. The bit error rate can be in principle reduced by implementing the error correction codes foreseen in the DVB-T standard.

2.2. Disturbance cancellation

The Extensive Cancellation Algorithm - Carrier and Doppler shift (ECA-CD [18]) has been used in order to effectively reduce the clutter contribution due to multipath. Specifically, in this work a multi-stage ECA approach has been applied. This means, the ECA filter is applied to the Doppler bin that collects the most interference power. Subsequently, the process is repeated on the output of the first ECA stage. In addition, the ECA filter is applied in the range frequency domain (that is, ECA-C) to account for different multipath/interference that may occur within the spectrum of the DVB-T signal. The further enhancement from ECA-C to ECA-CD expands the clutter subspace in the Doppler domain. This is done by adding replicas of the reference signal shifted by fractions of the Doppler resolution bin (typical values are Doppler frequencies $f_{ECA-CD} = \pm 0.75$ Hz). Further details can be found in [18].

2.3. Bistatic range-velocity map evaluation

The evaluation of the bistatic range-velocity map is the key step of each PCL processing [3]. It is well known that its purpose is to recognise weak target contributions in the surveillance signal, delayed and Doppler shifted. In the present implementation, the range-velocity map is calculated based on the periodic structure of the DVB-T signal.

Namely, for each DVB-T OFDM symbol the synchronization to the transmitter, decoding and remodulation of the DVB-T symbol is performed. Then, always at DVB-T symbol level, the reconstructed clean replica of the transmitted symbol is cross-correlated with the corresponding surveillance signal. This cross-correlation implements the so-called reciprocal filter [19], which equalizes the sub-carriers power over the DVB-T spectrum, and it performs a range compression of the single DVB-T symbol. It is easy to show that the reciprocal filter leads to a flat spectrum before final range inverse Fourier transform, thus minimizing spurious peaks in the resulting map. After that, the range compressed DVB-T symbols are juxtaposed in the slow-time (i.e. in the coherent integration time interval) and finally a discrete Fourier transform is performed to synthesize the Doppler dimension that can be then easily mapped into a corresponding velocity axis. The output of this stage is a bistatic range-velocity map $\chi[r, v]$ in which targets' echoes and disturbance sources are included. The latter ones may include, besides thermal noise, cancellation residuals and interferences. These contributions might severely affect each map by increasing its background level, thus limiting the detection of targets' echoes. For instance, for a FM radio based PCL system it has been shown that the disturbance level may be enhanced up to 15-20 dB above the nominal system noise level [13]. Moreover this effect might significantly vary with time and with the adopted surveillance antenna polarization.

3. Polarimetric detection schemes

In a conventional single-pol operation (namely L=1 in Fig. 1), once the bistatic range-velocity map has been evaluated, a Cell Average-Constant False Alarm Rate (CA-CFAR) threshold can be applied to detect targets with a given probability of false alarm. In contrast, when multiple receiving channels are connected to differently polarized surveillance antennas, various approaches can be considered to jointly exploit the outputs of the L polarimetric channels, according to the assumptions that are made on the disturbance statistical properties. The two detection schemes considered in this paper are described in sub-sections 3.1 and 3.2.

3.1. Polarimetric-Non Coherent Integration (P-NCI)

Let us consider the bistatic range-velocity maps obtained at the L polarimetric surveillance channels, $\chi_l[r, v]$ ($l = 1 \dots L$). For a given Cell Under Test (CUT) at range bin r_0 and velocity bin v_0, the results of the L channels are collected in a complex vector $\mathbf{x}_0 = [\chi_1[r_0, v_0] \dots \chi_L[r_0, v_0]]^T$. In the following, we assume that target echoes at the L polarimetric channels have unknown complex amplitudes, i.e. $\mathbf{x}_0 = \mathbf{s} = [\alpha_1 \dots \alpha_L]^T$ in the

absence of interference, where α_l is the unknown complex amplitude of the target at the l-th polarimetric channel. Let us make the simplifying assumption that the interference affecting different channels is statistically Independent and Identically Distributed (IID). In addition, let us assume $\mathbf{x}_0$ to follow a complex normal distribution with zero mean vector under hypothesis H_0 (disturbance only) and mean vector $\boldsymbol{s}$ under hypothesis H_1 (disturbance plus target) and covariance matrix $\sigma^2\mathbf{I}_{L\times L}$, being σ^2 the interference power on the single polarimetric channel, and being $\mathbf{I}_{L\times L}$ the identity matrix of size L. The assumption of a Gaussian distributed disturbance affecting each map is widely adopted in the technical literature especially when dealing with low resolution radar systems. In particular, recent studies have shown that it is a quite accurate assumption to describe clutter echoes in passive radar based on DVB-T signals, even in coastal scenarios [20]-[21]. Moreover we observe that a Gaussian distributed background is here assumed to properly describe the overall disturbance contributions that typically include both clutter echoes and interference from other transmitters. Under these hypotheses, a quite effective approach to enhance the SINR on the target is to resort to a NCI across polarimetric channels [12] . Specifically, the outputs obtained at the L polarimetric channels are incoherently summed after square law detector:

$$z[r_0, v_0] = \|\mathbf{x}_0\|^2 = \sum_{l=1}^{L} |\chi_l[r_0, v_0]|^2 \tag{1}$$

Then, assuming that the interference is (locally) homogeneous on the integrated range-velocity map, aiming at detecting the target presence, a CA-CFAR detection scheme can be adopted against the integrated map. To this purpose, we define a set $I_{[r_0,v_0]}$ of Q indices that identify range-velocity bins surrounding the CUT ($\mathrm{z}[r_q, v_q]$, $q \in I_{[r_0,v_0]}$, $|I_{[r_0,v_0]}| = \mathrm{Q}$). The average intensity estimated over these Q secondary bins is used to scale the result of (1), before thresholding:

$$\frac{\mathrm{z}[r_0, v_0]}{\sum_{q\in I_{[r_0,v_0]}} \mathrm{z}[r_q, v_q]} \underset{H_0}{\overset{H_1}{\gtrless}} G \tag{2}$$

The threshold G can be found by numerically inverting the following expression of the theoretical false alarm probability ($\mathrm{P_{FA}}$) [12]:

$$P_{FA} = \sum_{l=0}^{L-1} \binom{QL + l - 1}{l} \left(\frac{G}{QL}\right)^l \left(1 + \frac{G}{QL}\right)^{-QL-l} \tag{3}$$

where the integration stage over multiple receiving channels has been properly taken into account [7].

The advantages of the P-NCI scheme have been studied in [12] and [15] for the FM radio and the DVB-T cases, respectively. Specifically, these advantages are mainly due to the target echo enhancement resulting from the NCI of its contribution on different channels. In addition, some benefits are provided by the capability to average the severe interference in bad polarimetric channels with that appearing in the good ones, thus reducing its impact on the final performance.

However, in [12]-[13] we observed that, when a NCI scheme is adopted within an FM radio based passive radar system, the capability to control the actual false alarm rate was often jeopardized. This revealed the weakness of the hypothesis we have made concerning the statistical independence of the disturbance affecting different polarimetric channels. For the above reasons, an alternative technique has been introduced in [13], aiming at fruitfully exploiting the polarization diversity to reject the disturbance contributions that might limit the achievable detection performance.

3.2. Polarimetric-Generalized Likelihood Ratio Test (P-GLRT)

By admitting that the disturbance limiting the target detection is mainly related to external sources (e.g. clutter cancellation residuals, co-/adjacent-channel interferences, etc.), such disturbance cannot be assumed uncorrelated between different polarimetric channels. Moreover, based on the assumption that the target polarimetric characteristics might be very different from the disturbance, a P-GLRT detection scheme has been derived in [13], able to exploit the polarimetric differences and to improve the target discrimination capability.

To this purpose, complex vector $\mathbf{x}_0$, collecting as before the L polarimetric channels outputs at the CUT, is assumed to follow again a complex normal distribution with mean vector $\gamma\mathbf{s}$ under hypothesis H_γ (with γ=0, 1), but it has now a non-diagonal covariance matrix $\boldsymbol{D}$. In addition, a set of Q secondary vectors, $\mathbf{x}_q$ $(q = 1,..,Q)$, are made available, which contain the output of the L maps at range-velocity locations adjacent to the CUT, i.e. $\mathbf{x}_q = [\chi_1[r_q, v_q]\ \ \chi_2[r_q, v_q] \cdots \chi_L[r_q, v_q]\ ]^T$. They are assumed to be IID with the same statistic of $\mathbf{x}_0$ under hypothesis H_0. By resorting to the GLRT approach in [22], the detection test [13] is obtained:

$$\mathbf{x}_0{}^{\mathrm{H}}\widehat{\mathbf{D}}^{-1}\mathbf{x}_0 \underset{H_0}{\overset{H_1}{\gtrless}} \lambda \tag{4}$$

where $\widehat{\boldsymbol{D}} = \sum_{q=1}^{Q} \mathbf{x}_q\mathbf{x}_q^H$ is the sample covariance matrix and λ is the threshold.

The threshold can be properly selected according to the theoretical expression of the P_{FA} in [13] :

$$P_{FA} = \frac{(1-\eta_0)^{Q-L+1}}{(Q-L)!} \sum_{j=1}^{L} \frac{(Q-j)!}{(L-J)!} {\eta_0}^{L-j} \tag{5}$$

being $\eta_0 = \lambda Q/(Q+\lambda)$. As is apparent from (4) the P-GLRT approach can be interpreted as the cascade of a whitening transformation followed by a NCI of the whitened output. Therefore it still benefits from the integration of target echoes across different polarimetric channels. However, differently from P-NCI, it has the additional capability to reject the disturbance contributions (i.e. cancellation residuals or co-/adjacent- channel interfering transmissions) limiting the PCL performance. The above advantages have been extensively demonstrated in [13] for a FM-based PCL system. Specifically, the proposed P-GLRT has been shown not only to provide better results than a single a priori fixed polarization but also to yield a remarkable improvement with respect to the NCI approach. Therefore there is a great interest in understanding whether the above characteristics could provide similar benefits also in DVB-T based PCL systems.

4. Acquisition campaign

The experimental data set considered in this paper has been collected during a field trial conducted in 2014 on September, the 24th in Eckernförde, Germany. A map of the area where the experimental campaign took place is reported in Fig. 2. It also sketches the adopted acquisition geometry and the paths of the moving objects employed. Specifically, their trajectories during the whole test are represented in dotted lines, while the portions of the trajectories exploited in this work are represented in bold continuous lines.

4.1. DVB-T based passive radar setup

The exploited illuminator of opportunity is located in Kiel (approximately 20 km away from the receiver site) and broadcasts DVB-T signals in a single frequency network. It is working in 8k transmission mode, with 6817 OFDM carriers employed, in a 16-QAM (Quadrature Amplitude Modulation) scheme and a guard interval of 1/4. We used the DVB-T signal broadcasted at 666 MHz with an Equivalent Radiated Power (ERP) of 47 kW. Further details about the transmitter of opportunity are listed in Table 1 The experimental passive radar system PARASOL [16] developed at Fraunhofer FHR was employed. It consists of two parallel receiving channels, the receiver front-end and the data and signal processing unit (see Fig. 3).

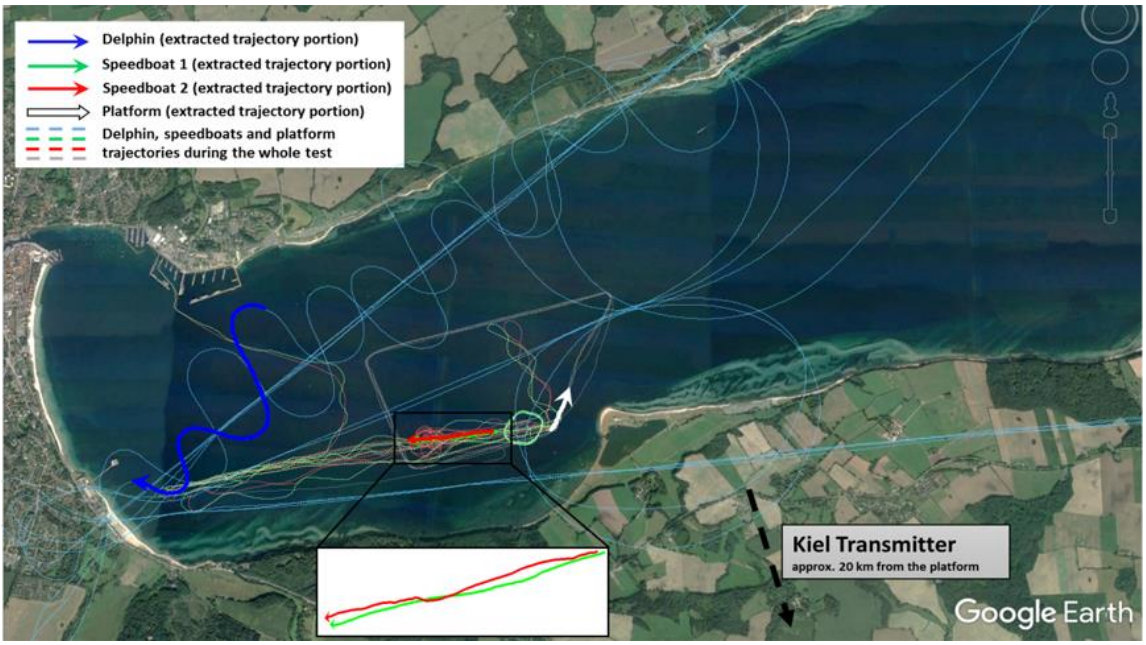

Fig. 2 *Acquisition geometry. Trajectories of the three cooperative targets and the platform are sketched: dotted lines represent the path during the whole test; bold continuous lines represent the extracted portions used in this work*

Pre-processing of the data includes synchronization to the transmitter, demodulation/remodulation of the DVB-T signal, and range compression through reciprocal filter as briefly discussed in Section 2 (see also [23]). For the purpose of our analysis, the two available channels were connected to two cross-polarized antennas. In particular two linearly polarized log-periodic antennas have been used, manufactured by Schwarzbeck, with a gain of 7 dBi in the frequency band under test during the trials (see more specifications in Fig. 3 (a)). The antennas were spaced approximately one meter apart[1] and rotated by 90 degrees one to the other, so as to collect the horizontally and vertically polarized versions of the received echoes. The system PARASOL was mounted on a moving platform (namely a military boat about 15 meters long), describing a trapezoidal loop in the fjord, as shown in dotted grey in Fig. 2. However, during the acquisition period reported in the following, it approximately moved on a rectilinear trajectory covering a global distance of 500 m (see the bold white portion of the trajectory in Fig. 2) .

4.1. Adopted methodology

In this paper, the results are reported for 168 consecutive data files, for a total acquisition duration of approximately 96 seconds.

[1] An antenna spacing of approximately one meter has been proven to adequately limit antenna coupling effects for these specific antennas at this range of operating frequencies in preliminary anechoic chamber measurements.

Table 1 Main parameters of DVB-T transmitter in Kiel

Position (WGS-84)	10°60'6.2"E 54°18'2.3"N
Modulation	16-QAM
Site Elevation [m] / Antenna Height [m]	38/ 219
Frequency [MHz]	666
ERP [kW]	47
Transmitted polarization	Horizontal

All the available data files have been processed according to the basic DVB-T based PCL processing scheme described in Section 2. Then the polarimetric detections schemes illustrated in Section 3 have been applied and their results are compared to those obtained with a single-polarization (shortened to single-pol in the following) operation using either the Vertical (V) or the Horizontal (H) polarimetric channel separately. Being interested in the detection capability provided by different approaches, the attention is focused on the results obtained against a few cooperative targets. Specifically, one ultra-light aircraft and two identical speedboats have been employed as cooperative targets. Table 2 shows some technical details of the aircraft Delphin (see Fig. 4 (a)) from Fraunhofer FHR. The true trajectory of Delphin during the whole test is reported in Fig. 2 (in dotted light blue) as provided by the Global Positioning System (GPS) receiver on-board. The availability of truth-data for the cooperative targets allowed us to evaluate the performance of the PCL system, in terms of number of correct detections. We recall that the bold continuous portion of the trajectory in Fig. 2 corresponds to the acquisition interval considered in this paper. The speedboats are two identical 7 m long rubber boats (see Fig. 4(b)), equipped with GPS receivers. Their true trajectories are reported in Fig. 2 in green and red, respectively.

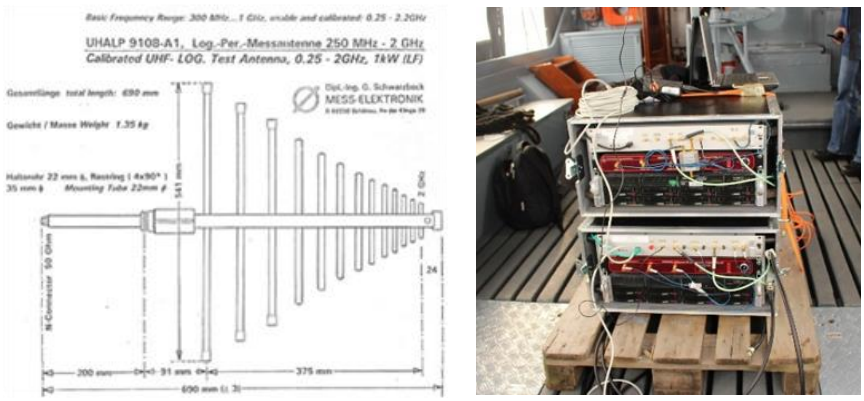

a b

Fig. 3 *Sketch of PARASOL system:*
a Antenna unit
b Data and signal processing unit

Table 2 Delphin aircraft technical details

Motor	Rotax 912 ULS
Art	4-Zylinder Boxer
Revolutions Per Minute (RPM)	5800
Tank capacity	120 liter
Service ceiling	3000 m
Top speed	260 km/h
Cruise speed	180 km/h
Stall speed	65 km/h
Empty weight	295 kg

Since the two speedboats navigated very close to each other during the whole test, their trajectories largely overlap. In particular, during the acquisition period considered in this paper (see the zoom in Fig. 2), they describe half period displaced sinusoids around a common rectilinear trajectory, moving away from the receiver platform. Based on the a priori knowledge of the bistatic geometry, the available target true trajectories are projected onto the bistatic range-velocity plane. This allows a direct comparison with the plots provided by the PCL sensor. See for example Fig. 5 where the bistatic trajectories of Delphin and of the two speedboats are reported as blue, red, and green continuous lines, respectively. Therefore a given PCL plot obtained at a specific data file is declared to be a “correct detection” when it appears at the expected bistatic range-velocity location occupied by one of the cooperative targets at the considered time instant.

a

b

Fig. 4 *Cooperative Targets*
a Delphin aircraft
b One of the speedboats

To make the procedure robust to the inaccuracies of both the PCL measurements and the GPS data projection onto the bistatic plane, proper confidence intervals in range (±100 m) and velocity (±3 m/s) have been defined for the described association stage. With this counting procedure, reasonably accurate estimates of the detection rate can be obtained because, when the false alarm rate is kept sufficiently low, it is very unlikely to include false plots within the correct detections. The results are reported in Section 5.

5. Results against experimental data

By recalling the processing scheme depicted in Fig. 1, two sets of results are reported in the following sub-sections. Specifically, in sub-section 5.1, we have initially considered the possibility of removing the disturbance cancellation stage separately performed at each polarimetric channel. Subsequently, in sub-section 5.2, we have repeated the detection performance analysis, after the application of the disturbance cancellation scheme illustrated in sub-section 2.2.

5.1. Results obtained without disturbance cancellation at each channel

The experimental test considered in this paper is representative of a short range surveillance application against both aerial and maritime targets. In such conditions the capability to limit the computational load required to attain given performance might be a key point as it in principle enables a real time operation and, consequently, fast reaction times. To this purpose, we considered the possibility of avoiding a dedicated disturbance cancellation stage to be separately applied at each receiving channel. This turns out to be a challenging condition in which the considered polarimetric schemes could be interestingly tested. In fact, in the absence of a preliminary cancellation stage, the detection of potential targets competes with the high power direct signal and multipath returns that spread over the range-velocity maps. Therefore, we report the detection results obtained when skipping the disturbance cancellation block in Fig. 1. The two remaining processing stages of Fig. 1 (direct signal reconstruction and bistatic range-velocity map evaluation) have been regularly applied against the received data. In particular, four different approaches have been employed at the target detection stage: (i) single-pol operation using the horizontally polarized channel only (single-pol H), (ii) single-pol operation using the vertically polarized channel only (single-pol V), (iii) P-NCI, and (iv) P- GLRT. In Fig. 5 we report on the bistatic plane the raw detection results obtained after each approach, compared to the GPS based trajectories available for the three cooperative targets.

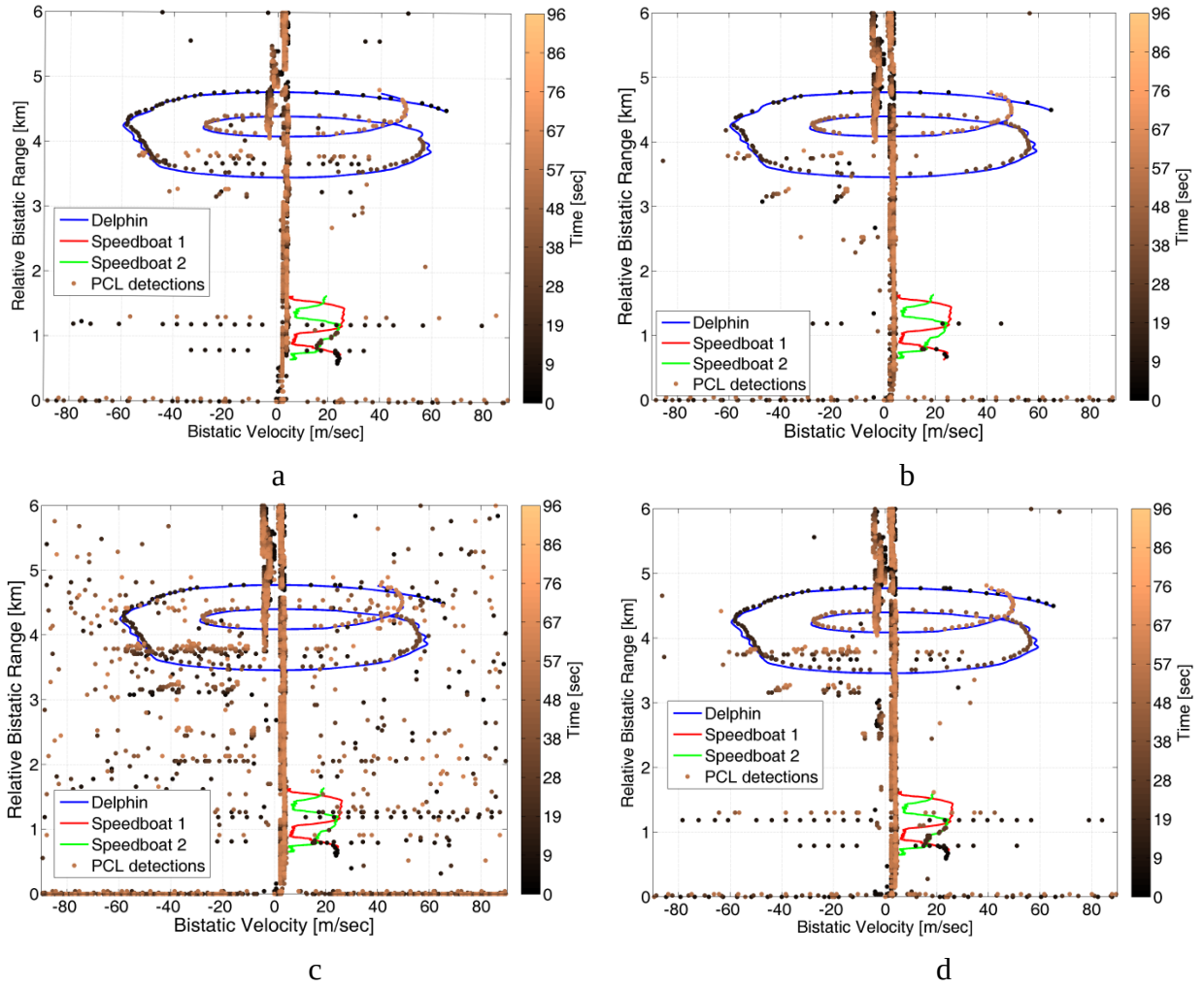

Fig. 5 *Detection results in the range-velocity plane, without applying any cancellation stage, for 168 consecutive scans, (approximately 96 seconds), for* $\boldsymbol{P_{FA} = 10^{-6}}$*. The temporal information is mapped in brown graduating shade. Different detection schemes are used in the following sub-figures:*

a single-pol H
b single-pol V
c P- NCI
d P-GLRT

Specifically, the relative bistatic range axis represents the path transmitter-target-receiver, minus the baseline, while the bistatic velocity represents the absolute sum of the radial velocities of all moving objects. In fact, the returns from stationary clutter appears slightly Doppler shifted. The raw detections collected for the 168 consecutive data files, are reported as brown plots in a common plane. The temporal information is mapped in brown graduating shades, starting from the darkest one (see colorbars in Fig. 5 and in Fig. 6). For all the considered detection schemes, the threshold has been set in order to obtain a nominal $P_{FA} = 10^{-6}$. Correspondingly, for each approach, we report in Table 3 the number of correct detections provided against the three cooperative targets. We briefly recall the counting procedure, explained in sub-section 4.1.

For each data file, a PCL plot is considered a "correct detection" when its bistatic range-velocity location is coincident with the location of cooperative target at the considered time instant. Proper confidence intervals in range and velocity have been defined for the described association stage to make it robust to inaccuracy. In Table 3, also the results obtained with different setting of the nominal P_{FA} are reported for an extended performance comparison. Based on the results in Fig. 5 and Table 3, the following considerations are in order:

(i) The use of a single-pol operation leads to quite different results depending on the polarization of the employed antenna. This is well in line with the results in [12]-[13], [15]. Specifically, for this particular data set we can say that, on average, the single-pol H yields better results in terms of number of correct detections against all the three targets considered. Incidentally, we recall that the exploited IO uses horizontal polarization. Nevertheless, this trend is not stable and it may change with time. Namely, the single-pol V occasionally provides correct detections at scans where the single-pol H experiences a missed detection (see for example the Delphin tracks portion between 4-4.2 km and 40-60 m/s, in Fig. 5 (a) and (b)). This can be explained by observing that the targets' echoes typically show a random polarization due to the reflection of the transmitted signal on the complex structures of the targets.

(ii) A P-NCI approach only allows to slightly increase the number of correct detections against the aerial target Delphin with respect to the best performing single-pol channel. Furthermore the advantage gets smaller as the P_{FA} decreases and this shows that, despite the target echoes integration, the resulting SINR did not improve because of a corresponding increase in the interference background level. Similarly, the P-NCI does not succeed in enhancing the detection capability against the small maritime targets. For instance, for Speedboat 2, the performance of the P-NCI is much more comparable with that provided by the worst single-pol channel. In addition, it is worth noticing that a considerably higher number of false alarms appears in the considered range-velocity area, as it has been originally verified for the case of FM radio based PCL in [13]. The inability to provide an effective control of the false alarm rate can be mostly attributed to the weakness of the hypothesis of statistical independence of the disturbance affecting the L different range-velocity maps. This especially applies to the case study under consideration since, in the absence of a prior disturbance cancellation stage, the observed interference is mainly due to the direct signal from the transmitter and its multipath replicas.

(iii) The P-GLRT detection scheme yields the best performance thanks to its capability to adaptively reject the disturbance contribution based on the polarimetric information.

Table 3 Number of correct detections obtained for the three cooperative targets with different polarimetric detection schemes using different P_{FA} values in the absence of a prior cancellation stage.

cooperative target	Delphin				Speedboat 1				Speedboat 2			
$\boldsymbol{P_{FA}}$	single pol H	single pol V	P-NCI	**P-GLRT**	single pol H	single pol V	P-NCI	**P-GLRT**	single pol H	single pol V	P-NCI	**P-GLRT**
10^{-5}	134	121	142	**149**	14	3	14	**17**	19	4	5	**22**
10^{-6}	131	114	140	**145**	11	3	10	**13**	16	2	4	**21**
10^{-7}	130	107	134	**142**	10	1	8	**11**	14	1	4	**16**
10^{-8}	127	97	131	**142**	7	0	6	**10**	9	1	4	**10**

Specifically, the P-GLRT allows to increase the number of correct detections with respect to both the best performing single-pol channel and the P-NCI, for all the three cooperative targets included in the analysis. This represents a clear advantage as it enhances the continuity of the obtained plot sequences that potentially simplifies a subsequent track initiation stage. Also, compared to P-NCI, P-GLRT allows to effectively control the false alarm rate. It is worth noticing that the plots formations outside the targets trajectories are rarely due to the homogeneous background. They are rather due to the sidelobes of high power zero-Doppler contributions (severe multipath and/or interfering transmitters) or, eventually, to other targets of opportunity.

5.2. Results obtained after disturbance cancellation at each channel

Results analogous to those reported in Fig. 5 and Table 3 are shown in Fig. 6 and Table 4 when including the disturbance cancellation stage in the basic processing chain of the DVB-T based PCL system. Specifically, the disturbance cancellation has been implemented according to the ECA-CD approach described in sub-section 2.2.

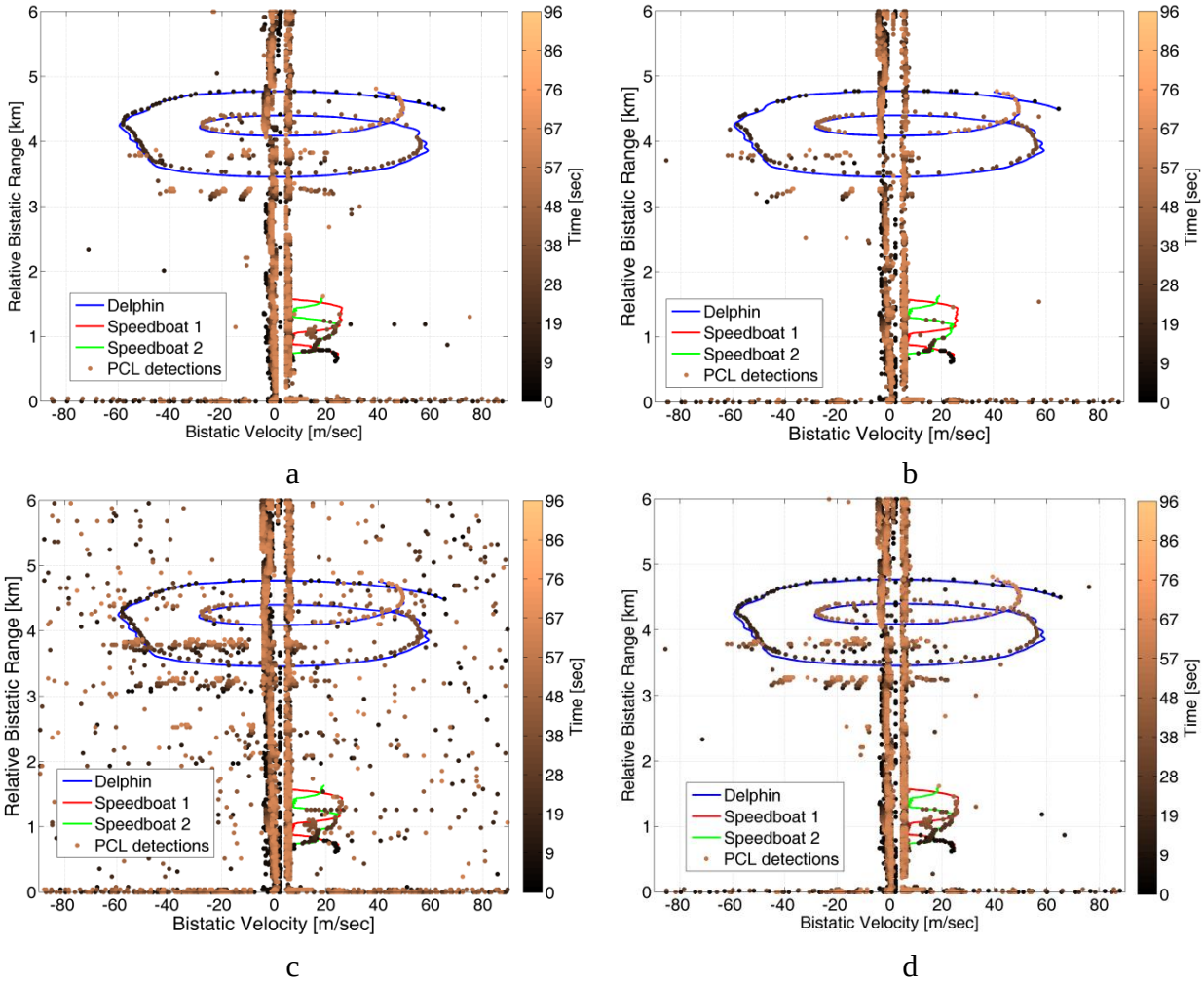

Fig. 6 *Detection results in the range-velocity plane, after applying a 2 stages ECA-CD algorithm, for 168 consecutive scans, (approximately 96 seconds), for* $\boldsymbol{P_{FA} = 10^{-6}}$*. The temporal information is mapped in brown graduating shades. Different detection schemes are used in the following sub-figures:*

a single-pol H
b single-pol V
c P- NCI
d P-GLRT

Two stages of the algorithm were sufficient to mitigate the limited clutter Doppler spread mainly caused by the receiver platform slow motion. As is apparent, all the considered polarimetric detection schemes benefit from the prior cancellation stage separately applied at each polarimetric channel and thus provide improved performance with respect to the corresponding results discussed in sub-section 5.1. This is particularly evident for the speedboats' tracks that were almost entirely hidden behind the strong stationary disturbance, when not removed in a prior stage. This is quite apparent in Fig. 7 that reports the range-velocity maps obtained for the single-pol H at a given scan. Specifically, in Fig. 7 (a-b) the results are reported before and after applying a 2-stages ECA-CD, respectively.

.

Table 4 Number of correct detections obtained for the three cooperative targets with different polarimetric detection schemes using different P_{FA} values, after the application of a 2-stages ECA-CD.

cooperative target	Delphin				Speedboat 1				Speedboat 2			
P_{FA}	single pol H	single pol V	P-NCI	**P-GLRT**	single pol H	single pol V	P-NCI	**P-GLRT**	single pol H	single pol V	P-NCI	**P-GLRT**
10^{-5}	143	125	144	**152**	36	17	32	**42**	56	25	46	**59**
10^{-6}	141	117	144	**150**	26	11	27	**37**	50	20	40	**56**
10^{-7}	137	109	139	**149**	24	7	25	**31**	46	18	38	**51**
10^{-8}	135	103	137	**148**	16	7	18	**24**	42	16	33	**45**

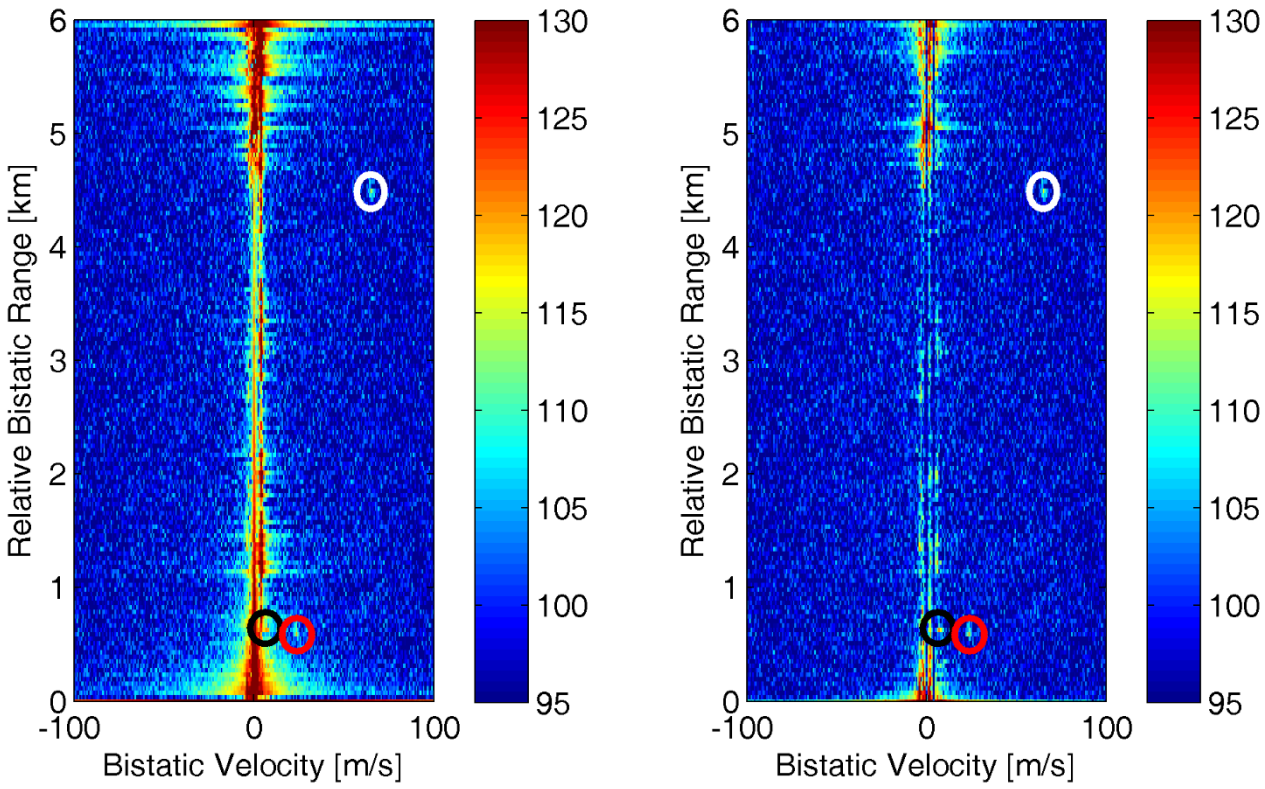

a b

Fig. 7 *Range-velocity maps for single-pol H, single scan, before thresholding:*
a without a 2-stages ECA-CD
b after a 2-stages ECA-CD

While Delphin appears as a strong peak in both cases (see the circles at approximately 4.4 km), the stationary disturbance severely masks the weak echoes of the speedboats that, at this scan, are located at approximately 0.6 km. After the removal of the disturbance contributions around the zero Doppler, the speedboats yields isolated peaks that can be successfully detected against the low power level background. Therefore, when collecting the results at consecutive scans, a greater number of correct detections are obtained after the application of the ECA-CD with all the considered polarimetric schemes. Also, some of the undesired plots formations that were present in Fig. 5 have been correctly removed in Fig. 6 as they were probably originated by stationary disturbance contributions. Despite this overall improvement, the comparative analysis presented in sub-section 5.1 among the different polarimetric detection schemes is entirely confirmed here. Specifically, the P-NCI still suffers from a limited capability of controlling the false alarm rate In fact, even after the ECA-CD application, the presence of cancellation residuals of other sources of externally generated interference might jeopardize the hypothesis of uncorrelated disturbance contributions at the available polarimetric channels. The P-GLRT still offers the best results after the stationary disturbance has been strongly reduced. This underlines that, when avoiding the prior cancellation stage, the P-GLRT scheme has the potential to mitigate the strongest interference contribution caused by the direct signal and its multipath replicas. On the other hand, when these contributions have been largely reduced by a dedicated processing stage, the P-GLRT approach still allows to enhance the resulting performance by counteracting possible cancellation residuals or other interference sources.

In this regard, we report in Fig. 8 the direct comparison of the results obtained with the single-pol operation (both H and V) after the 2-stage ECA-CD (see Fig. 8(a-b)) with the results of the P-GLRT either in the absence or after a prior cancellation stage (see Fig. 8(c-d)). In this case, the attention is focused on the correct detections only, so that the sequence of corresponding velocity measurements (black dots) is compared to the bistatic velocity tracks of the cooperative targets as a function of time. These figures allow to appreciate the continuity and the accuracy of the information provided by the PCL system employing different processing schemes. Incidentally, we observe that true target trajectories fluctuate due to the rough velocity estimation obtained via a differentiation of the range information provided by the GPS. Based also on the comparison of the numerical results reported in Table 3 and Table 4, we observe that when the P-GLRT scheme is applied without any prior cancellation stage (Fig. 8(c)), it provides better detection performance against the aerial target than the single-pol channels after the application of a 2-stage ECA-CD.

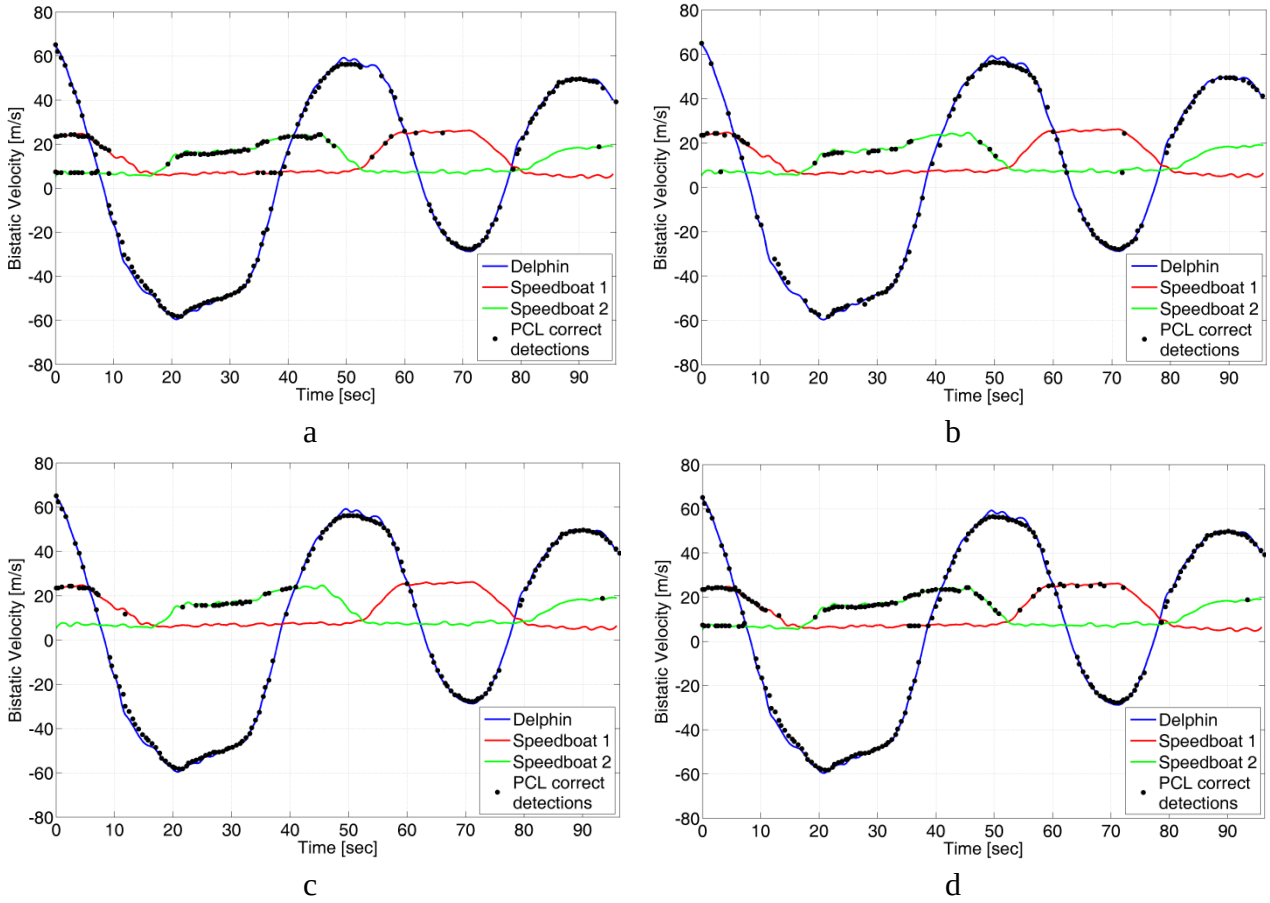

Fig. 8 *Extracted sequence of correct detections reported in the velocity-time domain for 168 consecutive scans (approximately 96 seconds) and nominal* $\boldsymbol{P_{FA} = 10^{-6}}$ *with:*
a single-pol H after a 2-stages ECA-CD
b single-pol V after a 2-stages ECA-CD
c P-GLRT without any prior cancellation stage
d P-GLRT after a 2-stages ECA-CD.

The advantage is tremendous with respect to the worst performing single-pol solution (i.e. single-pol V in Fig. 8(b)). In such a case, the polarimetric adaptive approach operating on the range-velocity map may constitute a valid alternative to the application of a cancellation stage in the signal domain. Clearly, the same conclusion cannot be drawn with reference to the small maritime targets as, in that case, the cancellation stage is strictly required for them to be detected with a reasonable detection probability. In such conditions, the additional disturbance rejection capability intrinsically provided by the P-GLRT might be a critical point. Comparing Table 3 and Table 4 it is apparent that the P-GLRT allows to increase the number of correct detections with respect to the best single-pol channel. For instance, with $P_{FA} = 10^{-6}$, an increase of 42% and 12% is observed against Speedboat 1 and Speedboat 2, respectively. If compared to the worst performing single-pol channel, the number of correct detections against the maritime targets is always more than tripled for Speedboat 1 and more than doubled for Speedboat 2.

The advantage of the P-GLRT is even more apparent if we observe that, in practical cases, it is difficult to identify an effective way of a priori establishing the best antenna polarization to be employed.

6. Conclusion

In this paper, following the successful results obtained for FM radio based PCL, the feasibility of a polarimetric operation is considered for passive radar exploiting DVB-T transmitters as illuminators of opportunity.

The results obtained using experimental data sets including cooperative targets allowed to prove the effectiveness of an adaptive approach to jointly exploit the information provided by two cross-polarized surveillance antennas.

In particular, the proposed P-GLRT detection scheme has been shown to guarantee:

i) enhanced detection capability with respect to the best performing single-pol channel;

ii) dramatically improved performance with respect to the worst performing single-pol channel;

iii) extremely better results with respect to the simple NCI of the information conveyed by the two single polarimetric channels.

7. References

[1] IEE Proceedings on Radar, Sonar and Navigation (special issue on passive radar systems), 153, 3 (June 2005).

[2] IEEE Aerospace and Electronic Systems Magazine (special issue on passive radar Part I & II), 27, 10-11 (2012).

[3] Lombardo,P., Colone,F.: 'Advanced processing methods for passive bistatic radar', in Melvin, W. L., and Scheer, J. A. (Eds.): 'Principles of Modern Radar: Advanced Radar Techniques' (Raleigh, NC: SciTech Publishing, 2012), pp. 739–821.

[4] Villano,M., Colone,F., Lombardo,P.: 'Antenna Array for Passive Radar: Configuration Design and Adaptive Approaches to Disturbance Cancellation', International Journal of Antennas and Propagation, 2013,16 pp.

[5] Zemmari,R., Broetje,M., Battistello,G., *et al.*: 'GSM passive coherent location system: performance prediction and measurement evaluation' IET Radar, Sonar & Navigation, 2014, **8** (2), pp. 94-105.

[6] Belfiori,F., Monni,S., Van Rossum,W., *et al.*: 'Antenna array characterisation and signal processing for an FM radio-based passive coherent location radar system', IET Radar, Sonar & Navigation, 2012, **6** (8), pp.687-696.

[7] Colone,F., Bongioanni,C., Lombardo,P.: 'Multifrequency integration in FM radio-based passive bistatic radar. Part I: Target detection', IEEE Aerospace and Electronic Systems Magazine, 2013, **28** (4), pp. 28-39.

[8] Colone,F., Bongioanni,C., Lombardo,P.: 'Multifrequency integration in FM radio-based passive bistatic radar. Part II: Direction of arrival estimation', IEEE Aerospace and Electronic Systems Magazine, 2013, **28** (4), pp. 40-47.

[9] Olsen,K.E., Woodbridge,K.: 'FM based passive bistatic radar target range improvement', Proc. Int. Radar Symp., Hamburg, Germany, September 2009.

[10] Olsen,K.E., Woodbridge,K., Andersen,I.A.: 'FM based passive bistatic radar target range improvement: Part II', Proc. Int. Radar Symp., Vilnius, Lithuania, June 2010.

[11] Son,I.-Y., Yazici,B.: 'Passive polarimetric multistatic radar for ground moving target', Proc. IEEE RadarConf. 2016, Philadelphia, PA, USA, May 2016, pp. 1-6.
[12] Colone,F., Lombardo,P.: 'Exploiting polarimetric diversity in FM-based PCL', Proc. IEEE International Radar Conference 2014, Lille, France, October 2014, pp. 1-6.
[13] Colone,F., Lombardo,P.: 'Polarimetric passive coherent location', IEEE Transactions on Aerospace and Electronic Systems, 2015, **51** (2), pp. 1079-1097.
[14] Colone,F., Lombardo,P.: 'Non-coherent adaptive detection in passive radar exploiting polarimetric and frequency diversity', IET Radar, Sonar & Navigation, 2016, **10** (1), pp. 15-23.
[15] Conti,M., Moscardini,C., Capria,A.: 'Dual-polarization DVB-T passive radar: Experimental results', Proc. IEEE RadarConf. 2016, Philadelphia, PA, USA, May 2016, pp. 1-5.
[16] Heckenbach,J., Kuschel,H., Schell,J., *et al.*: 'Passive radar based control of wind turbin collision warning for air traffic PARASOL', Proc. Int. Radar Symp. 2015, Dresden, Germany, June 2015, pp. 36-41.
[17] Searle,S., Howard,S., Palmer,J.: 'Remodulation of DVB-T signals for use in passive bistatic radar', Proc. of 44th Asilomar Conf. on Signals, Systems and Computers, Pacific Grove, CA, USA, Nov. 2010, pp. 1112-1116.
[18] Schwark,C., Cristallini,D.: 'Advanced multipath clutter cancellation in OFDM-based passive radar systems', Proc. IEEE RadarConf. 2016, Philadelphia, PA, USA, May 2016, pp. 1-5.
[19] Searle,S., Palmer,J., Davis,L., *et al.*: 'Evaluation of the ambiguity function for passive radar with OFDM transmissions', Proc. IEEE RadarConf. 2014, Cincinnati, OH, USA, May 2014, pp. 1040-1045.
[20] del-Rey-Maestre,N., Jarabo-Amores,M.P., Mata-Moya,D., *et al.*: 'Statistical analysis of UHF bistatic radar clutter in coastal scenarios', 2015 European Radar Conference (EuRAD), Paris, 2015, pp. 253-256.
[21] del-Rey-Maestre,N., Mata-Moya,D., Jarabo-Amores,M.P., *et al.*: 'MLP-based approximation to the Neyman Pearson detector in a terrestrial passive bistatic radar scenario', IEEE EUROCON 2015 - International Conference on Computer as a Tool (EUROCON), Salamanca, 2015, pp. 1-6
[22] Kelly,E.J.: 'An adaptive detection algorithm', IEEE Transactions on Aerospace and Electronic Systems, 1986, **22** (1), pp. 115-127.
[23] Palmer,J., Harms,H., Searle.S., *et al.*: 'DVB-T passive radar signal processing', IEEE Transactions on Signal Processing, 2013, **61** (8), pp. 2116-2126.